NOTES AND CORRESPONDENCE

Evidence for Low-Frequency Waves of Tropical Rainfall Inferred from Microwave Brightness Temperature

YE HONG AND HYO-SUK LIM*

Department of Meteorology, Texas A&M University, College Station, Texas

2 August 1993 and 30 November 1993

ABSTRACT

Evidence for the 30–60-day oscillation was found in the rainfall data that were retrieved from Special Sensor Microwave/Imager brightness temperatures from January to December 1989. Spectral analysis of daily rainfall showed that the strongest rainfall oscillations were located from 5°S to 5°N and extend from about 60°E to 180°. The oscillation propagated eastward at a speed of approximately 4 m s^{-1} along the equatorial Indian–western Pacific Ocean area. Northward propagation at a speed of about 1.5 m s^{-1} was also detected from 15°S to 30°N over the Indian Ocean between early May and late July.

1. Introduction

Since Madden and Julian (1971, 1972) found the 40–50-day oscillation in the zonal wind of the tropics, many efforts have been made to explore the characteristics, origin, and theoretical understanding of this oscillation. Zangvil (1975), Yasunari (1979, 1980), and Murayama (1982) reported the existence of quasi-40-day cloudiness oscillations over the summer monsoon region of east Asia and India and suggested that they may be related to those found by Madden and Julian. Based on the results from 1979 First GARP (Global Atmospheric Research Program) Global Experiment (FGGE), Murakami et al. (1984) found that the intensification of the 40–50-day oscillation is associated with the conversion from potential to kinetic energy. Lorenc (1984) showed that such a planetary-scale, eastward-propagating divergent wave existed for the entire FGGE year. Murakami and Nakazawa (1985) showed that monsoon activity over an equatorial area from 50° to 150°E is directly linked to the 40–50-day oscillation via the Pacific Walker circulation. Krishnamurti et al. (1985) examined the intraseasonal variability (ISV) of divergent circulation during the FGGE year and identified a planetary-scale, eastward-propagating divergent wave whose amplitude was largest during the summer over the Indian monsoon area. The northward propagation of a divergent wave over the Indian Ocean/subcontinent during summer was also noted. Ardanuy et al. (1990) examined the 30–60-day mode of the monsoon using cloud cover and earth radiation budget data from the *Nimbus-7* satellite. They found the clear evidence of a 30–60-day oscillation and the eastward propagation of this oscillation. These authors suggested that the 40–50-day oscillation was linked to regional characteristics such as monsoon onsets, breaks, and fluctuations of low-level jets over India and Southeast Asia.

The global nature of the oscillation is revealed by studies of long-term records of wind and radiation data. Weickmann et al. (1985) and Knutson et al. (1986) reported possible relationships of tropical convection with global-scale circulation anomalies in the 30–60-day timescale. Lau and Chan (1983a,b) first noted large fluctuations in east–west dipole anomalies in monthly means of outgoing longwave radiation (OLR) over the Indian Ocean and the western Pacific. This was later found to be connected with the large persistence of the 40–50-day oscillation. In a series of papers, they subsequently documented the relationship between the global 40–50-day waves and the regional characteristics of the winter and summer monsoon, and the wintertime extratropical circulation anomalies (Lau and Chan 1985, 1986a; Lau and Phillips 1986). It was also pointed out that because of the similar spatial and relative temporal evolution of atmospheric anomalies associated with the 40–50-day oscillation and those with El Niño/Southern Oscillation (ENSO), the two phenomena may be closely related (Lau 1985a,b; Lau and

* Current affiliation: NASA/Goddard Space Flight Center, Greenbelt, Maryland.

Corresponding author address: Ye Hong, Department of Meteorology, Texas A&M University, College Station, TX 77843-3150.

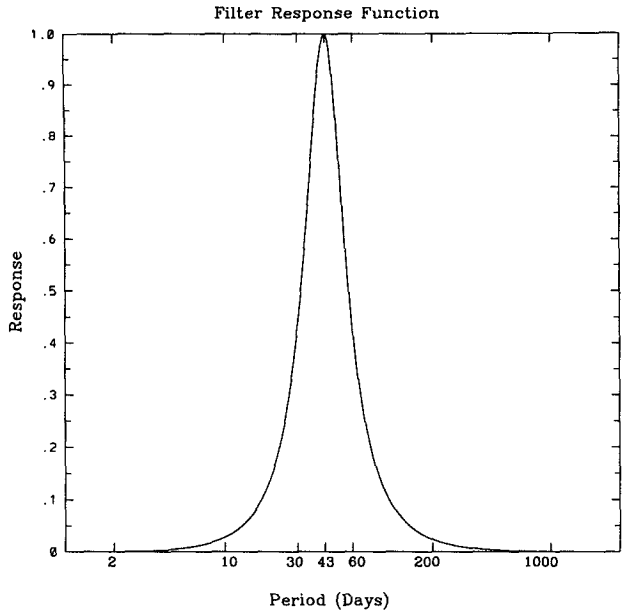

FIG. 1. Response function of a bandpass filter. It peaks at a period of 43 days and has half-power points at 30 and 60 days.

Chan 1986b). Lau and Chan (1987) also suggested that the onset of ENSO may be triggered as a result of the 40–50-day oscillation amplifying episodically through coupled air–sea interaction. The possibility of the 40–50-day oscillation as a trigger to ENSO is further supported by the systematic frequency and amplitude modulation of these oscillations before and after the 1982/83 ENSO.

Although the previous studies mainly focused on data sources consisting of OLR, cloudiness, zonal wind, temperature, and pressure fields, Singh and Kripalani (1985, 1986) have shown northward propagation of precipitation anomalies with a recurrence period of about 40 days across India during the summer monsoon season. Hartmann and Michelsen (1989) also demonstrated that the rainfall exhibited a statistically significant spectral peak at about 40 days over most of the southern half of India during summer. Yip and North (1993) found the eastward movement of the precipitation wave with a period of 50 days using an all-land version of the Community Climate Model developed at the National Center for Atmospheric Research. Lim (1993) also detected the 40–50-day oscillation of rainfall derived from the *Nimbus-5* Electrically Scanned Microwave Radiometer. As is well known, rainfall plays a very important role in atmospheric circulation. It is the primary exchange process within the hydrological cycle, and its latent heat release is a main driver of circulations in both the atmosphere and oceans. Additionally, rainfall is always observed in the summer monsoon. This suggests that the study of rainfall data will help us understand better the regional and global nature of the oscillation. In this paper, our main concern is determining whether or not the 30–60-day (or 40–50 day) oscillation and the propagation of this oscillation exist in rainfall data retrieved from microwave brightness temperatures.

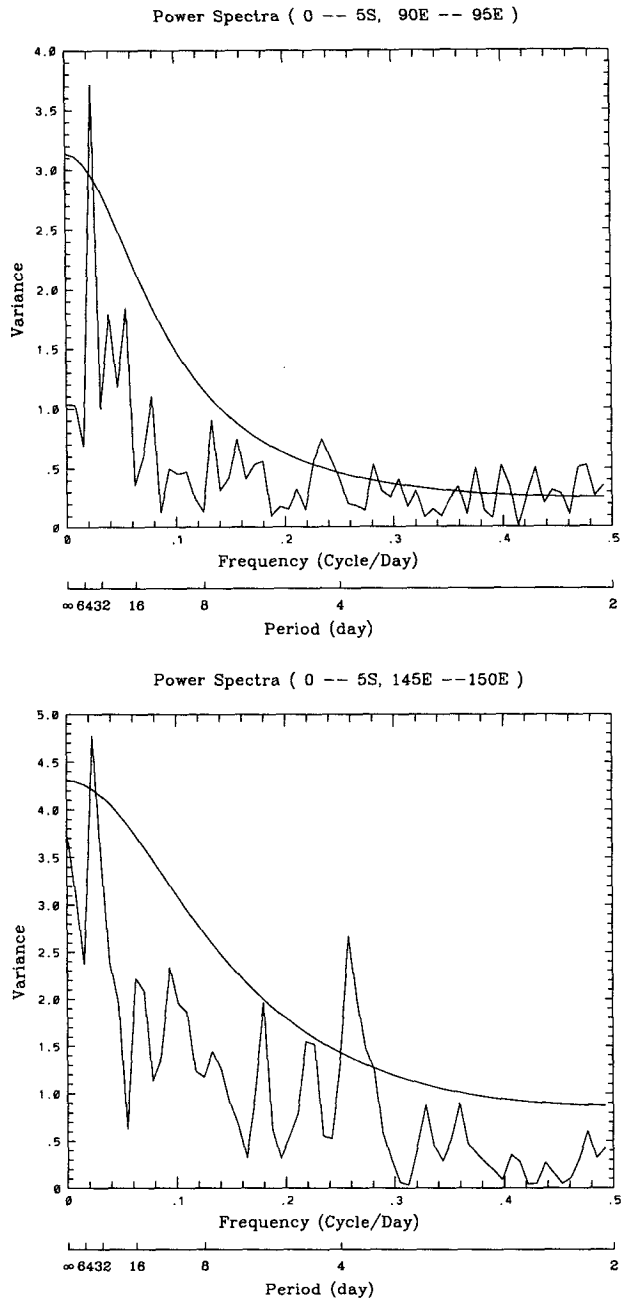

FIG. 2. Power spectra of daily rainfall for the regions (a) 0°–5°S, 90°–95°E; (b) 0°–5°S, 145°–150°E. Variance is in units of millimeters squared per spectral estimate. The smooth lines are 95% confidence levels for spectral peaks assuming a red noise null hypothesis.

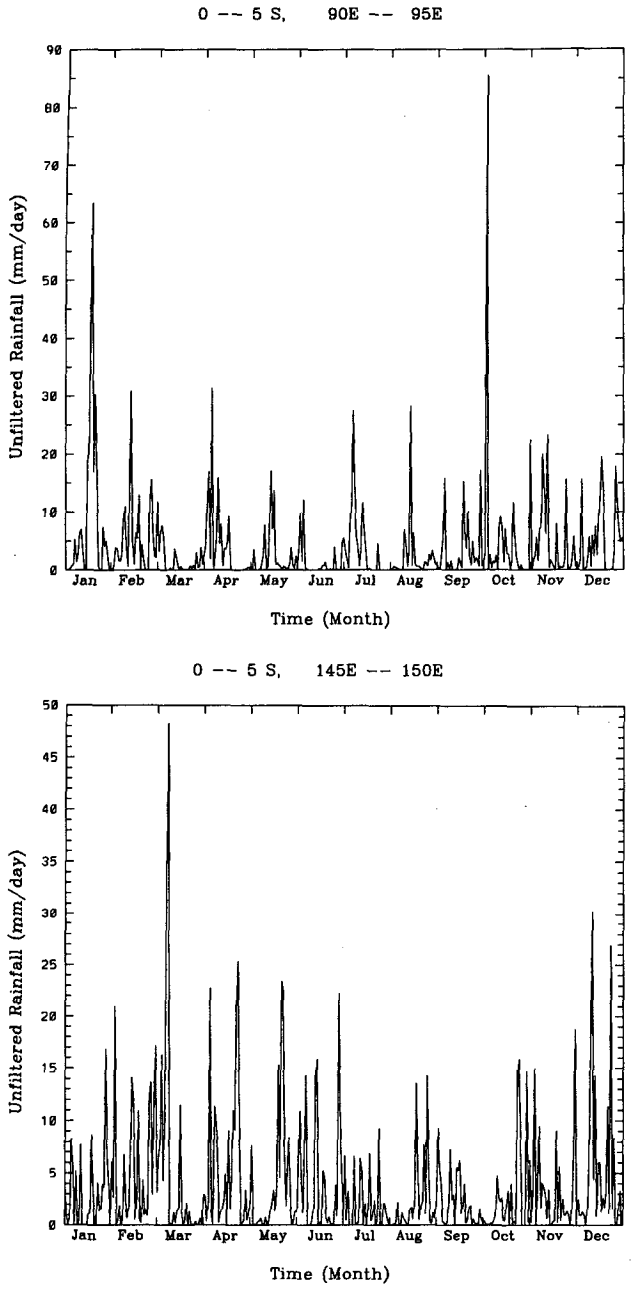

FIG. 3. Time series of unfiltered rainfall for the same regions as in Fig. 2.

We discuss the data and analysis in section 2. Section 3 gives results, and conclusions are given in section 4.

2. Data and analysis

The data used for the present study are rainfall data that were retrieved from the brightness temperature using rain rate–brightness temperature (R–T) relationships [see Wilheit et al. (1991) for details of the algorithm]. The brightness temperature was observed from Special Sensor Microwave/Imager (SSM/I) on the Defense Meteorological Satellite Program polar-orbiting satellite. The rainfall datasets were generated daily on a 5° × 5° grid and covered a period from 1 January to 31 December 1989. Rainfall on the land was excluded (set to zero) because the retrieval algorithm is best suited for ocean background. Of the total 365

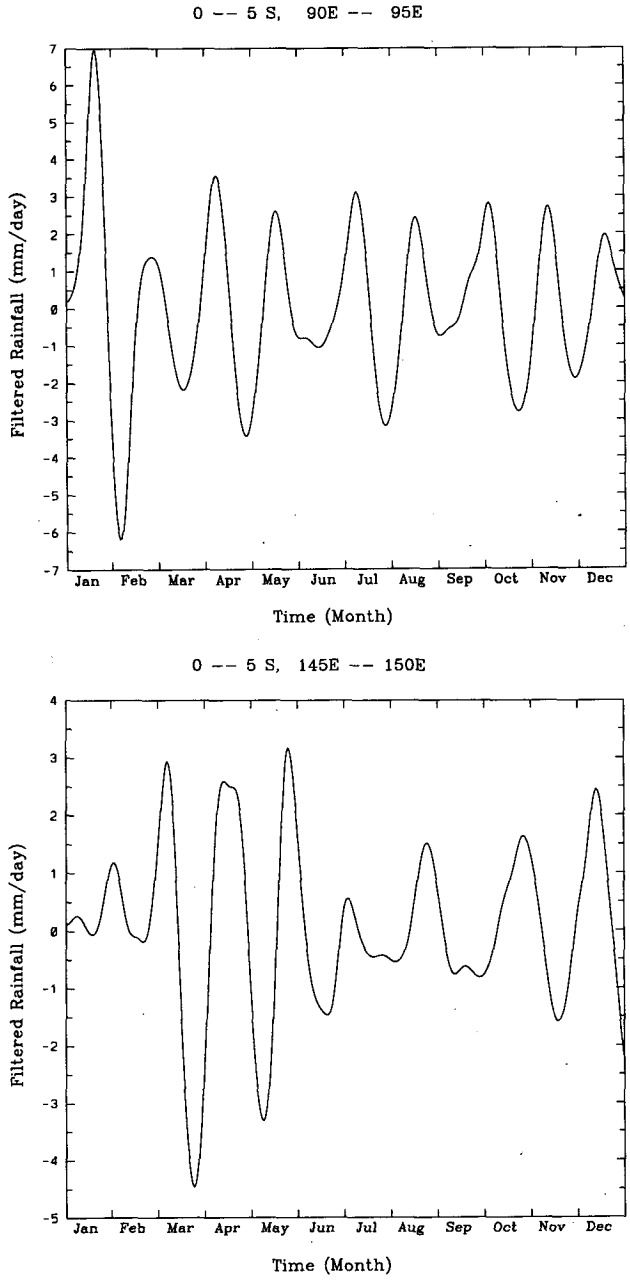

FIG. 4. Time series of filtered rainfall for the same regions as in Fig. 2. The negative values are caused by using a bandpass filter on the highly non-Gaussian rain field.

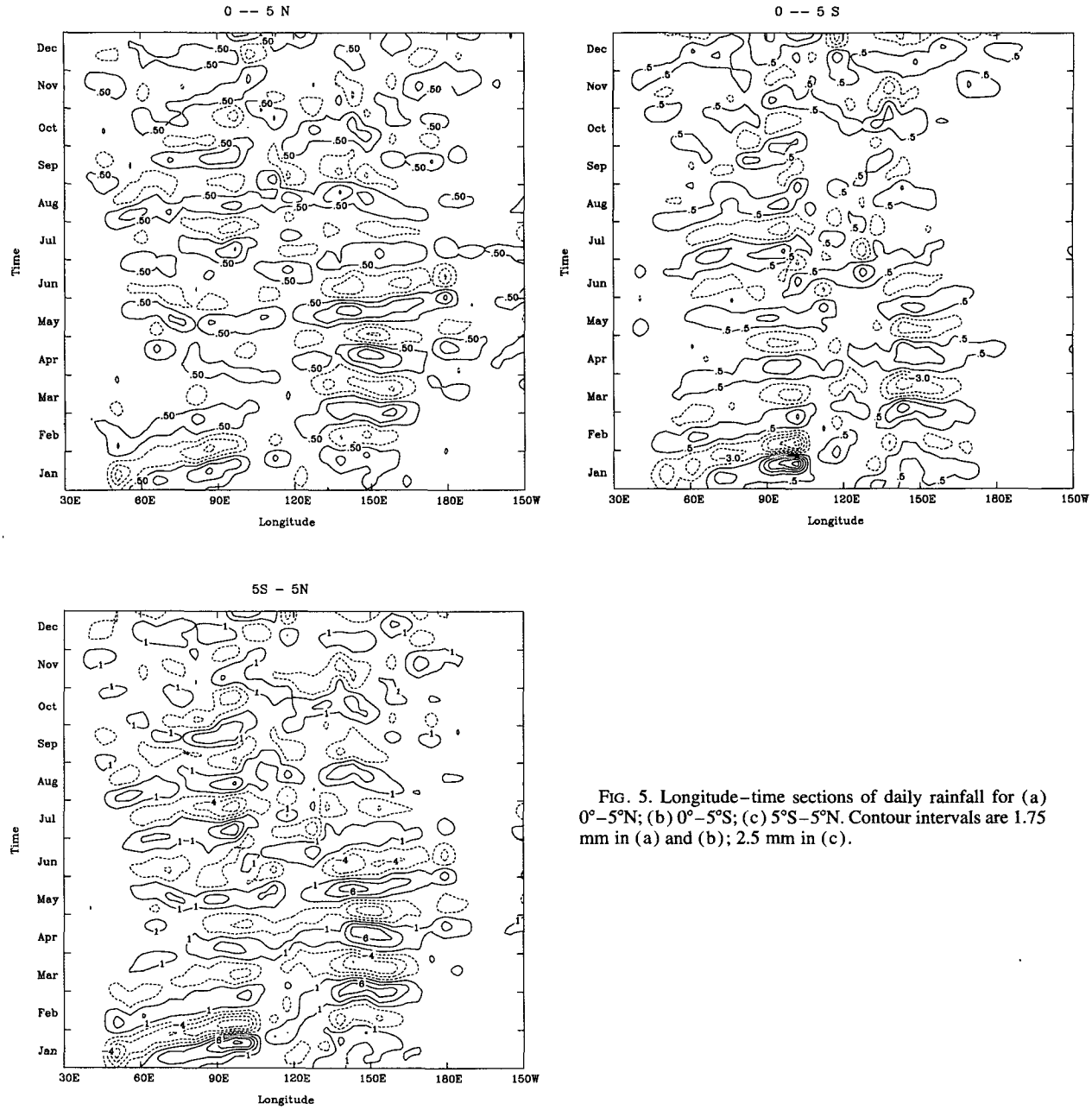

FIG. 5. Longitude–time sections of daily rainfall for (a) 0°–5°N; (b) 0°–5°S; (c) 5°S–5°N. Contour intervals are 1.75 mm in (a) and (b); 2.5 mm in (c).

days of data, 4 were missing and hence zeros were inserted.

Spectral analysis was performed on the rainfall time series data using a fast Fourier transform (Press et al. 1992) to determine the variance distribution of rainfall according to frequency band. Statistical significance tests were also performed on the rainfall variance using a red noise null hypothesis. To extract the signal of the 30–60-day oscillation, the data have been filtered with a recursive bandpass filter (Murakami 1979). The response function of the bandpass filter is presented in Fig. 1. It peaks at a period of 43 days and has half-power points at 30 and 60 days. The filtered time series were then used for the analysis of low-frequency waves.

3. Results

a. The 30–60-day oscillation

Figure 2 presents the power spectra for the unfiltered rainfall data of the regions over the equatorial Indian Ocean (0°–5°S, 90°–95°E) and the west Pacific (0°–5°S, 145°–150°E), respectively. The 95% confidence

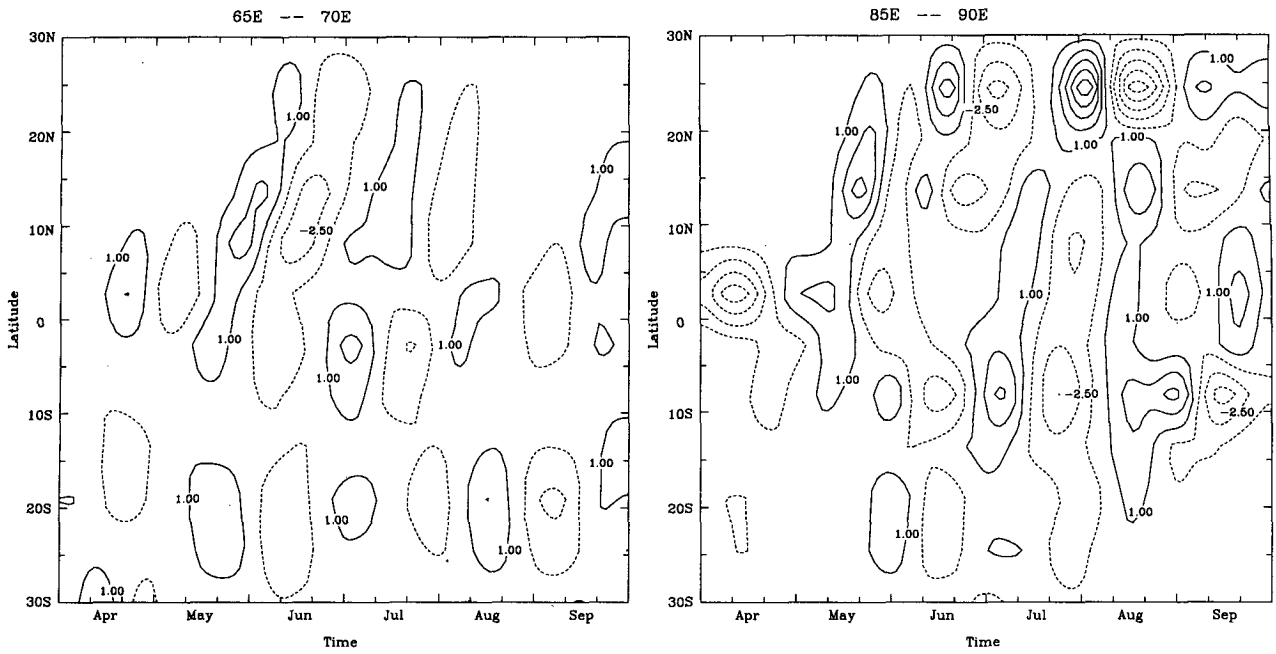

FIG. 6. Time–latitude sections of daily rainfall for (a) 65°–70°E; (b) 85°–90°E. The contour intervals are 1.75 mm.

levels for spectral peaks are also shown in Fig. 2, assuming a red noise null hypothesis. They both exhibit the statistically significant spectral peaks centered at the period of 43 days. We have performed the spectral analysis for the rainfall time series of all 5° × 5° grid elements from 50°S to 50°N. The spectral peaks with a period of 30–60 days can be found in most equatorial areas. This suggests that a low-frequency oscillation with periods of about 30–60 days exists in the tropical rainfall.

Figure 3 is the time series of unfiltered rainfall data in the same areas as in Fig. 2. The 30–60-day rainfall oscillations are clearly discernible. There are relatively large rainfalls that occurred around the middle of January and the beginning of October over the Indian Ocean (Fig. 3a) but around the beginning of March and the beginning of December over the west Pacific (Fig. 3b). Figure 4 is the time series of filtered rainfall data in the same areas as in Fig. 2. The negative values in Fig. 4 are caused by using a bandpass filter on the highly non-Gaussian rain field.

b. Propagation of oscillation

Krishnamurti and Subrahmanyan (1982), from an analysis of the 850-mb motion fields for the FGGE summer, showed the northward propagation of ridges and troughs from the equatorial Indian Ocean at a speed of 0.75° day^{-1}. Using the OLR data during the northern summer, Lau and Chan (1986) found an eastward-propagating, pulselike signal with a speed of about 3–4 m s^{-1} between 60°E and the date line. They also detected northward-propagating signals along 80°E, which migrated from 10°S to 25°N at a speed of 1–2 m s^{-1}. Both the eastward propagation along the equator and the northward propagation over the Indian subcontinent occur over an extended period well before the onset (late May to early June) and long after the withdrawal (late August to early September) of the Indian monsoon. Examining the 30–60-day mode of the monsoon using cloud and earth radiation budget data, Ardanuy et al. (1990) found that the speed of eastward propagation was 7.5°–8.5° day^{-1}, depending on the degree of activity of the monsoon.

To examine the propagation of the rainfall oscillation, longitude–time (x–t) and time–latitude (t–y) diagrams of filtered rainfall were made at different latitudes and different longitudes, respectively. Figures 5a, 5b, and 5c display the data in the zonal band 0°–5°N, 0°–5°S, and 5°S–5°N, respectively, between 30°E and 150°W for a 1-yr period. The eastward propagation can be clearly seen, and the velocity is estimated to be about 3.0°–4.5° day^{-1} (~3.5–5.0 m s^{-1}). These propagating rain fields seem to originate near 60°E over the Indian Ocean and vanish near the date line over the Pacific. The propagation feature is quite obvious from January to September but less obvious in the remaining months. After Figs. 5a and 5b were combined into Fig. 5c, the feature of eastward propagation became more distinct due to the improvement of ratio of signal to noise of the depiction.

Figures 6a and 6b show the time–latitude sections along 65°–70°E and 85°–90°E. The northward propagation of rainfall oscillation can be seen but it is only

for a limited period from the beginning of May to the end of July. This apparent propagation may be connected with the summer monsoon. Along the 65°–70°E, the oscillation propagates northward at the speed of about 1.30° day^{-1} (~1.5 m s^{-1}) from 10°S to 30°N. The northward propagation signal at the speed of about 1.80° day^{-1} (~2.0 m s^{-1}) is more clear along 85°–90°E from about 15°S to 30°N.

4. Summary and conclusions

The 30–60-day oscillation has been found in the rainfall data that were retrieved from SSM/I brightness temperatures in 1989. The oscillation propagated eastward at a speed of approximately 4 m s^{-1} along the equatorial India–western Pacific Ocean areas. Northward propagation at a speed of about 1.5 m s^{-1} was detected from 10°S to 30°N over the Indian Ocean from May through July.

The previous studies of the characteristics of the oscillation using a variety of data sources, observation periods, and analysis methods have shown that the low-frequency oscillation in the tropical atmosphere has a concentration of variance in a broad period range from 30 to 60 days. They have predominant zonal scales of wavenumbers 1 and 2, and propagate eastward along the equator. There is a marked northward propagation of disturbances over India and east Asia during the northern summer monsoon season. The results of the present study show that the rainfall data retrieved from microwave observations contain the basic features of the low-frequency oscillation observed previously by other means. This indicates that the 30–60-day rainfall oscillation found in this study is related to the global 40–50-day waves found by Madden and Julian (1972). However, whether there are relationships between this 30–60-day rainfall oscillation and the monsoon seasonal variation, the global circulation, or ENSO is still unknown. Longer records of microwave data are needed for further studies.

Acknowledgments. We wish to thank Dr. Thomas T. Wilheit and Dr. Gerald R. North for their guidance and encouragement, and their careful review of this manuscript. Thanks are due to Dr. James P. McGuirk, Dr. Jianping Huang, Yuhong Yi, and Capt. Don Conlee, and two anonymous reviewers for their helpful comments and their suggestions for improving the original draft of the paper. Thanks are also due to Alfred T. C. Chang for providing the SSM/I data tape. We also acknowledge the support from NASA by means of the TRMM science team and through Grant NAG5-1568.

REFERENCES

Ardanuy, P. E., C. R. Kondragunta, and H. L. Kyle, 1990: Low-frequency modes of the tropical radiation budget. *Meteor. Atmos. Phys.*, **44,** 167–194.

Bendat, J. S., and A. G. Piersol, 1971: *Random Data: Analysis and Measurement Procedure.* Wiley and Sons, 407 pp.

Cadet, D. L., 1986: Fluctuations of precipitable water over the Indian Ocean during the 1979 summer monsoon. *Tellus,* **38A,** 170–177.

Chen, T.-C., 1987: 30–50 day oscillation of 200-mb temperature and 800-mb height during the 1979 northern summer. *Mon. Wea. Rev.,* **115,** 1589–1605.

Hartmann, D. L., and M. L. Michelsen, 1989: Intraseasonal periodicities in Indian rainfall. *J. Atmos. Sci.,* **46,** 2838–2862.

Knutson, T. R., K. M. Weickmann, and J. E. Kutzbach, 1986: Global scale intraseasonal oscillations of outgoing longwave radiation and 250 mb zonal wind during the Northern Hemisphere summer. *Mon. Wea. Rev.,* **114,** 605–623.

Krishnamurti, T. N., and D. Subrahmanyan, 1982: The 30–50 day mode at 850 mb during MONEX. *J. Atmos. Sci.,* **39,** 2088–2095.

——, P. K. Jayakumar, J. Sheng, N. Surgi, and A. Kumar, 1985: Divergent circulations on the 30–50 day time scale. *J. Atmos. Sci.,* **42,** 364–375.

Lau, K. M., 1985a: Subseasonal oscillations bimodal climate state and the El Niño–Southern Oscillation. *Coupled Ocean–Atmosphere Model,* J. Nihoul, Ed., Elsevier, 29–40.

——, 1985b: Elements of a stochastic dynamical theory of the long-term variability of El Niño–Southern Oscillation. *J. Atmos. Sci.,* **42,** 1552–1558.

——, and P. H. Chan, 1983a: Short-term climate variability and atmospheric teleconnection as inferred from satellite derived outgoing longwave radiation Part I: Simultaneous correlations. *J. Atmos. Sci.,* **40,** 2735–2750.

——, and ——, 1983b: Short-term climate variability and atmospheric teleconnection as inferred from satellite derived outgoing longwave radiation Part II: Lagged correlations. *J. Atmos. Sci.,* **40,** 2751–2767.

——, and ——, 1985: Aspects of the 40–50 day oscillation during northern winter from outgoing longwave radiation. *Mon. Wea. Rev.,* **113,** 1889–1909.

——, and ——, 1986a: Aspects of the 40–50 day oscillation during the northern summer as inferred from outgoing longwave radiation. *Mon. Wea. Rev.,* **114,** 1354–1367.

——, and ——, 1986b: The 40–50 day oscillation and the El Niño–Southern Oscillation: A new perspective. *Bull. Amer. Meteor. Soc.,* **67,** 533–534.

——, and ——, 1987: Intraseasonal and interannual variations of tropical convection: A possible link between the 40–50 day oscillation and ENSO. *J. Atmos. Sci.,* **45,** 506–521.

——, and T. J. Phillips, 1986: Coherent fluctuations of extratropical height and tropical convection in intraseasonal time scale. *J. Atmos. Sci.,* **43,** 1164–1181.

——, and L. Peng, 1987: Origin of low-frequency (intraseasonal) oscillations in the tropical atmosphere. Part I: Basic theory. *J. Atmos. Sci.,* **44,** 950–972.

——, G. J. Yang, and S. H. Shen, 1988: Seasonal and intraseasonal climatology of summer monsoon rainfall over east Asia. *Mon. Wea. Rev.,* **116,** 18–37.

Lim, H. S., 1993: Rainfall estimation from ESMR-5 measurements and application to climate studies. Ph.D. dissertation, Texas A&M University, 146 pp.

Lorenc, A. C., 1982: The evolution of planetary-scale 200 mb divergent flow during the FGGE year. *Quart. J. Roy. Meteor. Soc.,* **110,** 427–441.

Madden, R. A., and P. R. Julian, 1971: Detection of a 40–50 day oscillation in the zonal wind in the tropical Pacific. *J. Atmos. Sci.,* **28,** 702–708.

——, and ——, 1972: Description of global scale circulation cells in the tropics with 40–50 day period. *J. Atmos. Sci.,* **29,** 1109–1123.

Murakami, M., 1979: Large-scale aspects of deep convective activity over the GATE area. *Mon. Wea. Rev.,* **107,** 994–1013.

——, 1984: Analysis of deep convective activity over the western Pacific and southeast Asia. Part II: Seasonal and intraseasonal variation during the northern summer. *J. Meteor. Soc. Japan,* **62,** 88–108.

Murakami, T., and T. Nakazawa, 1985: Tropical 45 day oscillations during the 1979 Northern Hemisphere summer. *J. Atmos. Sci.*, **42,** 1107–1122.

Murayama, T., 1982: Upper tropospheric zonal wind oscillation with a 30–50 day period over the equatorial western Pacific observed in cloud movement vectors. *J. Meteor. Soc. Japan,* **60,** 172–181.

Press, W. H., S. A. Teukolsky, W. T. Vetterling, and B. P. Flannery, 1992: *Numerical Recipes.* Cambridge Press, 963 pp.

Singh, S. V., and R. H. Kripalani, 1985: The south to north progression of rainfall anomalies across India during the summer monsoon season. *Pure Appl. Geophys.,* **123,** 624–637.

——, and ——, 1986: Application of extended empirical orthogonal function analysis to interrelationships and sequential evolution of monsoon fields. *Mon. Wea. Rev.,* **114,** 1603–1610.

Weickmann, K. M., G. R. Lussky, and J. E. Kutzbach, 1985: Intraseasonal (30–60 day) fluctuations of outgoing longwave radiation and 250 mb stream function during northern winter. *Mon. Wea. Rev.,* **113,** 941–961.

Wilheit, T. T., A. T. C. Chang, M. S. V. Rao, E. B. Rodgers, and J. S. Theon, 1977: A satellite technique for quantitatively mapping rainfall rates over the oceans. *J. Appl. Meteor.,* **16,** 551–560.

——, ——, and L. S. Chiu, 1991: Retrieval of monthly rainfall indices from microwave radiometric measurements using probability distribution functions. *J. Atmos. Oceanic Technol.,* **8,** 118–136.

Yasunari, T., 1979: Cloudiness fluctuations associated with the Northern Hemisphere summer monsoon. *J. Meteor. Soc. Japan,* **57,** 227–242.

——, 1980: A quasi-stationary appearance of 30–40 day period in the cloudiness fluctuations during the summer monsoon over India. *J. Meteor. Soc. Japan,* **58,** 225–229.

Yip, K. J., and G. R. North, 1993: Tropical waves in a GCM with zonal symmetry. *J. Climate,* **6,** 1691–1702.

Zangvil, A., 1975: Temporal and spatial behavior of large scale disturbance in tropical cloudiness deduced from satellite brightness data. *Mon. Wea. Rev.,* **103,** 904–920.